

Focus detection in digital holography by cross-sectional images of propagating waves

Meriç Özcan

Sabancı University
Electronics Engineering
Tuzla, İstanbul 34956, Turkey

ABSTRACT

In digital holography, computing a focused image of an object requires a prior knowledge of the distance of the object from the camera. When this distance is not known, it is necessary to repeat the image reconstruction at a range of distances followed by evaluation of each image with a sharpness metric to determine the in-focus distance of the object. Here, we present a method to find the focus distance by processing the image transverse to the object plane instead of the processing in the image plane as it is usually done. Since the reconstructed hologram image is spatially symmetric around the focus point along the propagation axis, simply finding the symmetry points in the image cross-section specifies the focus location, and no other sharpness metrics are necessary to use. Also with this method, it is possible to find the focus distances of multiple objects simultaneously, including the phase only objects without any staining. We will present the simulations and the experimental results obtained by a digital holographic microscope.

1. INTRODUCTION

Holographic imaging allows recording of a whole complex wave-field such that the phase and the intensity profile of the field could be recovered later. With the advancement of digital recording devices such as the charge-coupled devices (CCD), the field of digital holography was born, and since then one of the most important applications of holographic imaging has been in the microscopy field. Digital holographic microscopes (DHM) allow recording three dimensional information of objects and unlike the conventional microscopes, they can image transparent specimens without staining, and in addition, object focusing is not required while recording the holograms. Object image is recovered from the recorded holograms numerically by application of the diffraction integral which can be performed by various approaches such as the convolution, Fresnel transformation or the angular spectrum method.^{1,2} It is not necessary to focus the object image during the recording since the wave-field can be computed for any physical distance. However, computing an object's 3D profile with only a single reconstruction requires a prior knowledge of the distance of the object from the camera. When this distance is not known, it is necessary to repeat the image reconstruction at a range of distances, followed by evaluation of each image with a sharpness metric to determine the in-focus distance of the object.

The idea of using a sharpness metric to measure the in-focusness of an image was first proposed by Muller and Buffington³ in 1974. They suggested that a sharpness metric should produce a global maximum only for the image that is in focus. Common autofocus techniques applied in photography and microscopy today are based on successively evaluating the sharpness of the acquired images, and then by adjusting the lens or stage position to maximize the sharpness. There are numerous functions proposed in the literature for evaluating the sharpness of amplitude-only images.⁴⁻⁶ For example, variance based evaluation assumes that a focused image on the object plane will have higher contrast than a non-focused image. In the holography context, Langehanenberg⁷ and Memmolo⁸ investigated some gradient and variance based metrics. They both chose the normalized-variance metric as the most suitable choice for autofocusing in digital holography. Dubois⁹ analyzed the integral power of the hologram as a focus measure of pure-amplitude and pure-phase objects. Another metric that makes use of self-entropy is also proposed by Gillespie¹⁰ for assessing the sharpness of holograms. For faster autofocusing, it was also shown that scaled holograms can be used for estimating the true focus distance.¹¹

E-mail: meric@sabanciuniv.edu

Although the focus distance of a hologram can be estimated accurately by a focus metric, the overall process could be inconveniently slow when the size of the holograms are large. The reconstruction step in the sharpness curve calculation is the main bottle-neck of the process, and it might require special processors such as graphic processors to speed-up the calculations.¹²

2. FOCUS ESTIMATION BY SYMMETRY AT FOCUS

Focus estimation in general is an important problem for automated imaging applications, and adjusting the focusing in real time might be necessary to capture images with the highest quality. In digital holography, autofocusing problem is reduced to performing hologram reconstructions at several candidate distances and finding the location for the highest quality object image. A simple focus distance search algorithm would start by performing reconstructions at some distance range with a certain step size. It then applies a sharpness metric to the array of reconstructed images. The resulting array of the numbers is the sharpness curve of the image for that particular metric. The algorithm finally selects the distance with the maximum sharpness value -in which it could be a maximum or a minimum, depending on the method- as the object's focal distance from the camera. When a usual focus metric is applied to a reconstructed image, it is a global operation so that if there are multiple objects at different depths at the scene, it will not be possible to determine the depths of the objects with a single operation. One might need to apply focus metrics separately in local regions of the objects.

Here we propose a simple focusing technique which allows to determine focus depths from the cross section of the object intensity as the wave propagates. If we record the intensity of the wave transverse to the object plane as the wave passes through the focus point, it will be symmetric function. For example, Fig. 1 shows a hologram of a disk shaped aperture recorded at a certain distance away from the aperture. When the hologram is illuminated by a plane wave, the aperture is reconstructed at the same distance as used in the recording, and if we were to record the wave intensity in a plane transverse to the object plane that includes the propagation direction, we would see that the intensity of the wave would have been symmetric around the focus point. For the numerical

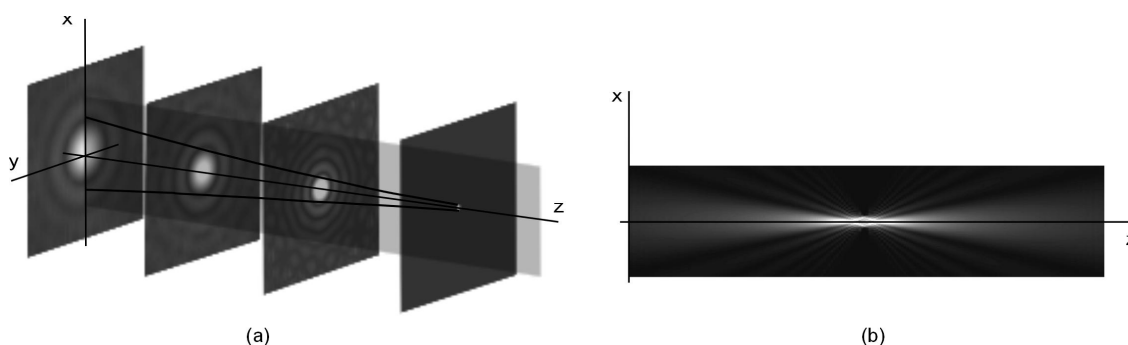


Figure 1. a) Reconstruction of a hologram of a circular aperture to show the focusing profile. Wave propagation is in the z direction. b) If we record the wave intensity in the xz plane as a function of distance z, the focus location will readily be identified due to symmetry of intensity around the focus point.

hologram reconstruction a variety of methods can be used such Fresnel transform, convolution method, or the angular spectrum method. For microscopy applications angular spectrum method is preferred since it does not have the minimum distance requirement. All of these methods involve discrete Fourier transforms (DFT). For example angular spectrum method uses two DFTs and a point-wise multiplication with the transfer function of free space. The method has an overall complexity of $\mathcal{O}(N^2 \log_2 N)$ for an image with $N \times N$ pixels, and as N increases the computational cost could become significant for a real-time system, and it may be necessary to use special hardware.¹²

3. SIMULATION RESULTS

A simple focus distance search algorithm with our method would start by performing reconstructions at some distance range with a certain step size. After selecting a region defined by a line on the reconstructed images, concatenation of the intensities of that line would produce the cross-sectional image. We will first demonstrate the method with Lena image which represents an amplitude object, later we will apply the method to pure phase objects. We assume holograms are recorded on-axis configuration, hence the wave propagation is perpendicular to the recording plane. However, the generalization of the method to off-axis recording is straightforward. Using

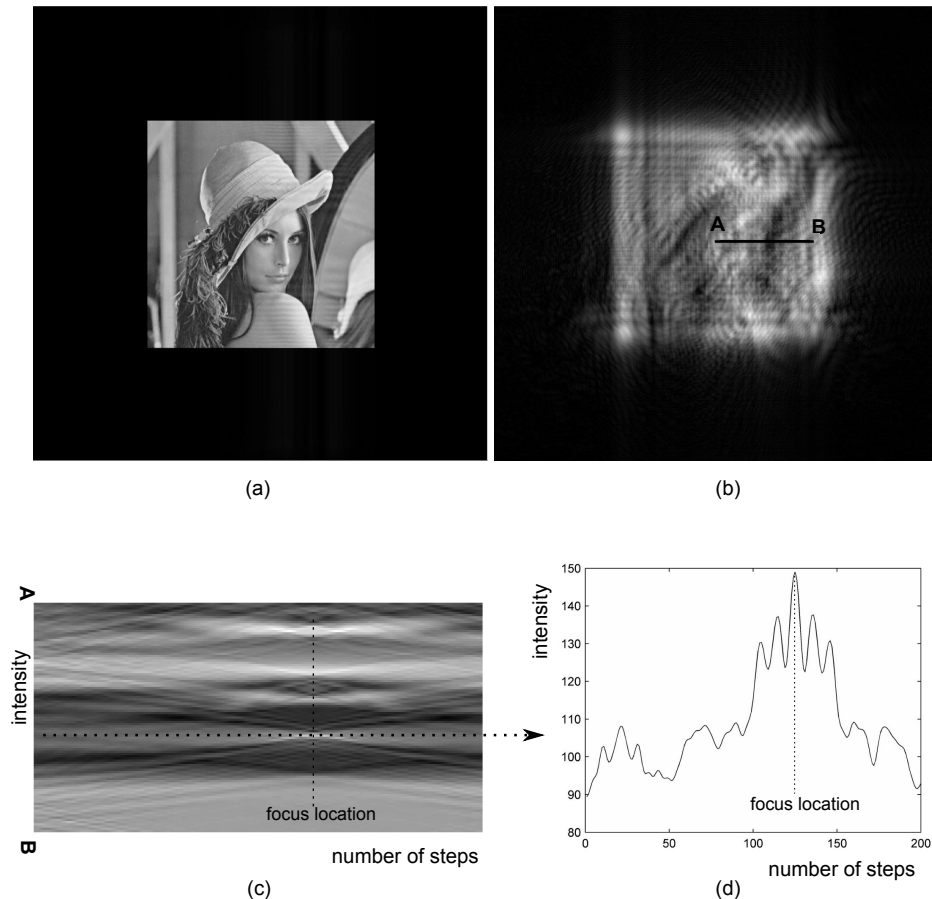


Figure 2. Simulation results with computer generated holograms. a) Lena image is used for the input object. It is zero padded to prevent aliasing due to FFT calculations. b) Far field is calculated by angular spectrum method, and the intensity of the object wave in the recording plane recovered from the hologram (using phase shifting holography technique) is shown. The line denoted with \overline{AB} (actually it is one pixel thick but shown here thicker for clear visualization) will be extracted from numerically reconstructed holograms. c) Cross-section image: Hologram is reconstructed 200 times (at each step propagation distance is increased by a constant amount), and the intensities of the image pixels defined by the line \overline{AB} are extracted and concatenated together. The resultant image is the cross section of the wave intensity, clearly symmetric around the focus location. d) One pixel of the line \overline{AB} -denoted with horizontal dashed line in the cross-section image- is plotted as a function of distance. Again, the focus location is clearly identified as the location of the symmetry.

the Lena image as the input object, far field is calculated by angular spectrum method, and the results are shown in Fig. 2 above. Here the Lena image is zero padded to prevent aliasing due to FFT calculations. We assume that the far field is calculated and added to a plane reference wave followed by the phase-shifting holography method^{12,13} to recover the object wave. Since everything is computer generated, we simply use the object wave information in the recording plane without actually calculating the hologram. By looking at the cross-section image, it is easy to locate the focus distance since the intensity is symmetric around the focus location. One

pixel of the reconstructed line -denoted with the dashed horizontal line in the cross-section image- as a function of distance is also shown. The symmetry around the focus point is clearly visible.

In the next simulation we used a computer generated hologram of two phase objects, a square and a circle shaped, located at different depths with respect to the recording plane. The Figure 3 shows the far field and the reconstructed holograms of the objects at their respective distances. Since they are phase objects, when they are reconstructed at their correct focus distances, they will not visible in the intensity images, and it is not easy to identify the object locations from the reconstructed images. However if we apply our method to this phase object hologram, focus locations of the objects will be identified readily from the cross-section image as demonstrated in Fig. 4. The intensity is symmetric around the actual focus distances, and one can immediately identify and determine the focus distances of both objects.

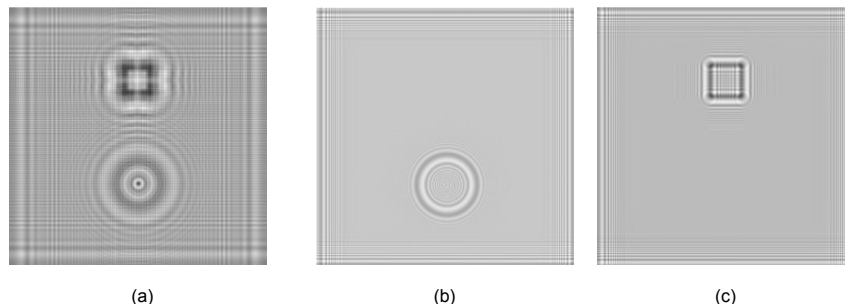


Figure 3. a) Far field intensity of a square and circular phase objects located at two different distances from the recording plane. b) Intensity of the reconstruction when the reconstruction distance is equal to the distance of the square. Only the diffraction pattern of the circle is visible since the square is in focus, and being pure phase object, it is not visible in the intensity image. c) This is the intensity of the reconstruction when the reconstruction distance is equal to the distance of the circle. Only the diffraction pattern of the square is visible, and now the circle is invisible.

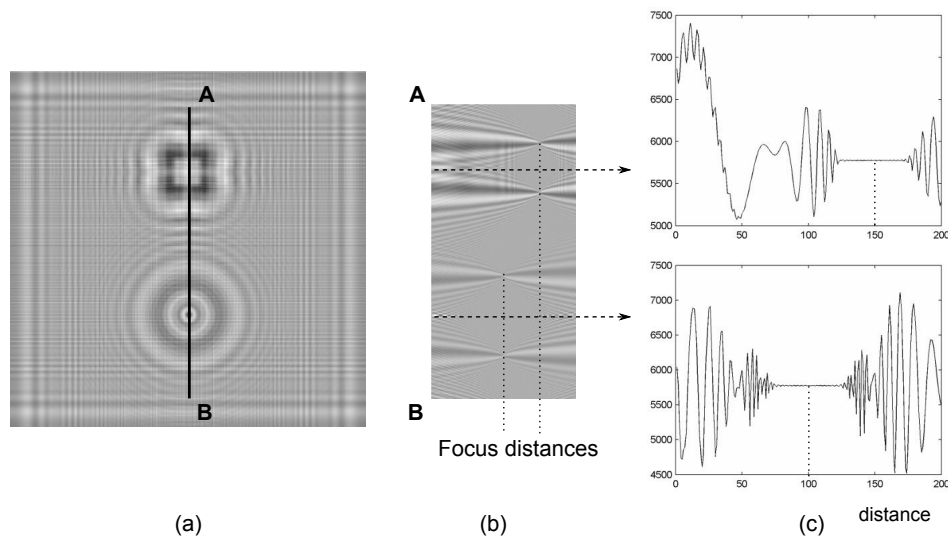


Figure 4. a) Far field intensity of a circle and a square phase only objects located at two different depths with respect to the recording plane. b) Cross-section image: Hologram is reconstructed 200 times by angular spectrum method (at each step propagation distance is increased by a constant amount), and the intensities of the image pixels defined by the line \overline{AB} are extracted and concatenated together. The resultant image is the cross-section image of the wave intensity transverse to the object plane, which shows the location of both objects as symmetric intensity variations. c) Two pixels of the line \overline{AB} -denoted with horizontal dashed lines in the cross-section image- are plotted as a function of distance. These figures correspond to the pixel intensity variations -which are the pixels centered at the corresponding objects- as the wave propagates. The symmetry around the focus points are clearly visible.

4. EXPERIMENTAL RESULTS

A transmission mode digital holographic microscope configured as a Mach-Zehnder interferometer is used in the experiments as shown in Fig. 5 below. A 5 mW, 762 nm solid-state laser is used as the light source. A beam-splitter splits the linearly polarized laser beam into an object arm and a reference arm. An opto-electronic phase

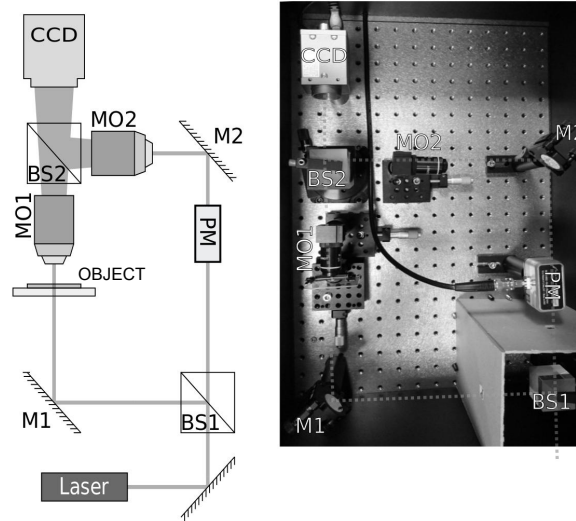


Figure 5. A schematic and a picture of the transmission based digital holographic microscope used in the experiments is shown. Before joining the two arms of the interferometer by BS2, object image is magnified by the microscope objective MO1 (NA=0.25). In order to compensate for the wave front curvatures, a similar objective MO2 is placed on the reference beam path.

modulator is used in the reference arm to modulate the phase of the reference wave to apply a phase-shifting holography technique. A second beam-splitter combines the reference wave and the object wave before the CCD, and this splitter is aligned for achieving on-axis hologram recording. The camera has 1024×1024 pixels with pixel dimensions of $3.75 \mu\text{m} \times 3.75 \mu\text{m}$. Microscope objectives and the object are all on adjustable translation stages such that target image can be located in front or behind the CCD recording plane ($\pm 6 \text{ cm}$). Microscope has lateral resolution of $2.2 \mu\text{m}$ in both axes, and the field of view is approximately 4.4 mm^2 .

A 1951 USAF resolution test chart etched on the metal layer of a glass substrate is used as the object for recording the holograms. Three different holograms of the object with a reference wave's phase of 0 , $\pi/2$, and π are recorded, and a phase shifting algorithm is applied to filter out the zero order and the conjugate images as described in detail elsewhere.¹² The recovered object wave and its reconstruction along a line is shown in Fig. 6. When closely inspected, cross-section image identifies two different focus distances for the top and bottom regions of the chart. For example group number 6 in the lower part is in focus when the reconstruction distance is 2.83 cm , and the group number 7 on the top portion is in focus when the reconstruction distance is 2.94 cm . This difference in focus distance immediately implies that the chart was not exactly parallel with respect to the recording plane. We suspect that with a conventional focus estimation method this difference will not be noticeable -unless each region is assessed locally-, and an average focus distance will be predicted. In order to test this idea and to compare focus finding capability of our method to a conventional method we did the following test: We chose normalized-variance method as the conventional focusing metric and used the same USAF hologram for the sharpness evaluation. The normalized-variance function as the sharpness measure was selected because it works very well most of the time. The principle of normalized-variance method relies on the fact that the magnitude images of the focused reconstructions will yield higher contrast than out-of-focus reconstructions, and by normalizing the variance of the image with its mean, images that contain abnormally high gray-level values are assigned lower sharpness values:

$$M_{var} = \frac{1}{\langle g \rangle} \sum \sum |g(x, y) - \langle g \rangle|^2, \quad (1)$$

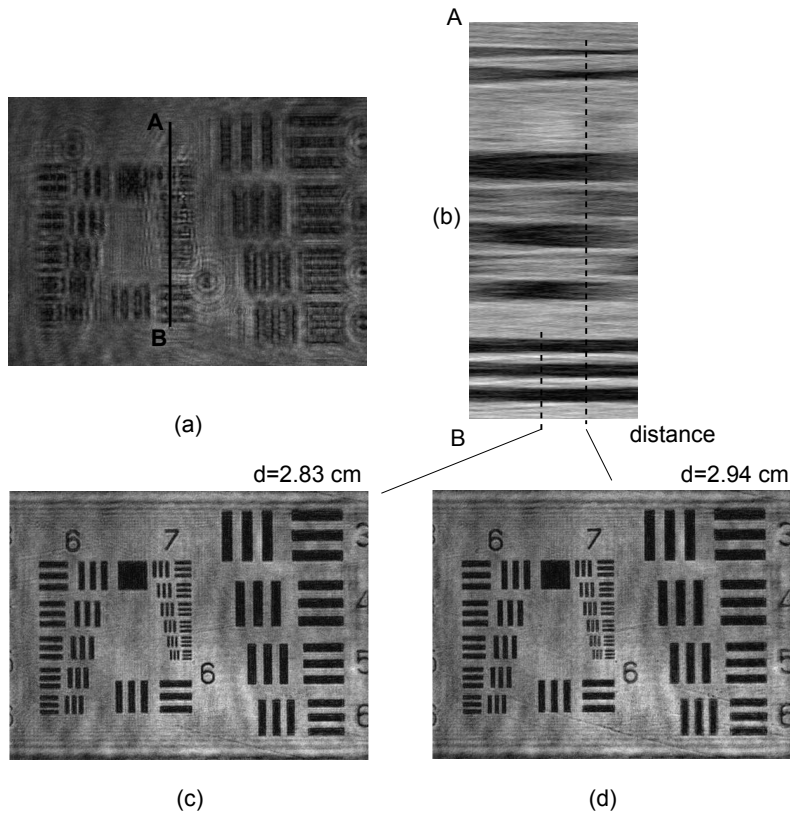


Figure 6. a) Recorded hologram where the pixels defined by the line \overline{AB} will be used to form the cross-section image. b) Cross-section of the wave intensity as a function of distance (again 200 reconstructions). There are two different focus locations are identified. c) For $d=2.83$ cm, the number 6 in the lower part of the chart is in focus. d) For $d=2.94$ cm, number 7 is in focus. This results shows that the test chart was not exactly perpendicular to the recording plane but was slanted slightly about the vertical axis.

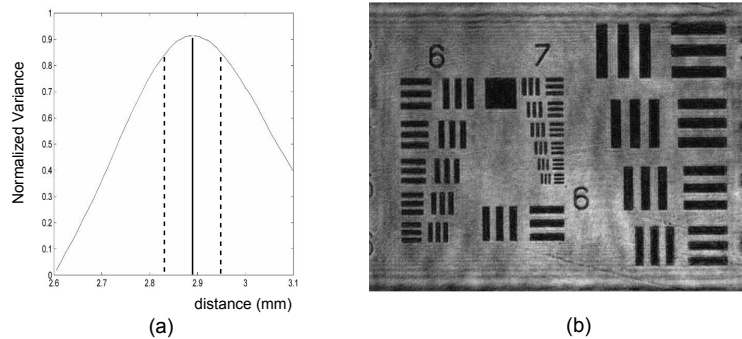


Figure 7. a) The hologram of USAF chart is reconstructed, and a sharpness value is calculated with normalized-variance metric for a range of distances. The maximum of the sharpness curve indicates the focus distance is about 2.89 cm. Dotted lines indicate focus distances that were calculated earlier with our cross-section image symmetry method. As expected, conventional method yielded sort of an average focus distance. b) Object image reconstructed at distance of 2.89 cm is shown. Close inspection shows that neither top nor bottom group numbers are at their maximum sharpness.

where, $g(x, y)$ denotes the intensity values of the image, $\langle g \rangle$ is the mean, and M_{var} is the calculated sharpness value of the image. We numerically reconstructed the hologram of USAF chart for a range of distances and at each distance a sharpness value is calculated given by Eq. 1. The results of this exercise is shown in Fig. 7. The maximum of the sharpness curve shows the focus distance as 2.89 cm, which is indicated by the solid line. Object image reconstructed at this distance is also shown, and here as expected, neither group number is quite in focus.

5. CONCLUSION

We presented a method to find the focus distance of objects in digital holography by finding the symmetry points in the cross-sectional images of propagating waves. Since the reconstructed hologram image is spatially symmetric along the propagation axis around the focus, simply finding the symmetry points in the image cross-section specifies the focus distance. No other focus metric is necessary to apply. With this method, it is possible to find the focus distances of multiple objects simultaneously including the phase only objects without any staining. We presented the simulations and the experimental results obtained by a digital holographic microscope which confirmed the method. We would like to note that this method is demonstrated for in-line hologram recording, but it can be extended to the off-axis recording in a straightforward manner. In that case the location of the line in the object plane will shift as the reconstructed wave travels at an angle with respect to the axis perpendicular to the hologram plane, which needs to be accounted for in the calculations.

ACKNOWLEDGMENTS

We thank to The Scientific and Technological Research Council of Turkey for funding this project (TÜBİTAK, project number: 110T613).

REFERENCES

- [1] Goodman, J. W., [*Introduction to Fourier Optics*], McGraw–Hill Companies, Inc., New York, second ed. (1996).
- [2] Özcan, M. and Bayraktar, M., “Digital holography image reconstruction methods,” *Proc. SPIE*, Vol. 7233, **72330B-1** (2009).
- [3] Muller, R. A. and Buffington, A., “Real-time correction of atmospherically degraded telescope images through image sharpening,” *J. Opt. Soc. Am.* **64**, 1200–1210 (1974).
- [4] Firestone, L., Cook, K., Culp, K., Talsania, N., and Preston, K., “Comparison of autofocus methods for automated microscopy,” *Cytometry* **12**, 195–206 (1991).
- [5] Groen, F. C., Young, I. T., and Lighthart, G., “A comparison of different focus functions for use in autofocus algorithms,” *Cytometry* **6**, 81–91 (1985).
- [6] Sun, Y., Duthaler, S., and Nelson, B. J., “Autofocusing in computer microscopy: selecting the optimal focus algorithm,” *Microscopy Research and Technique* **65**, 139–149 (2004).
- [7] Langehanenberg, P., Kemper, B., Dirksen, D., and von Bally, G., “Autofocusing in digital holographic phase contrast microscopy on pure phase objects for live cell imaging,” *Appl. Opt.* **47**(19), 176–182 (2008).
- [8] Memmolo, P., Distanti, C., Paturzo, M., Finizio, A., Ferraro, P., and Javidi, B., “Automatic focusing in digital holography and its application to stretched holograms,” *Opt Lett.* **36**, 1945 – 1947 (2011).
- [9] Dubois, F., Schockaert, C., Callens, N., and Yourassowsky, C., “Focus plane detection criteria in digital holography microscopy by amplitude analysis,” *Opt. Express* **14**, 5895–5908 (2006).
- [10] Gillespie, J. and King, R. A., “The use of self-entropy as a focus measure in digital holography,” *Pattern Recognition Letters* **9**(1), 19 – 25 (1989).
- [11] İlhan, H. A., Doğar, M., and Özcan, M., “Fast autofocusing in digital holography using scaled holograms,” *Optics Communications* **287**, 81–84 (2013).
- [12] Doğar, M., İlhan, H. A., and Özcan, M., “Real-time, auto-focusing digital holographic microscope using graphics processors,” *Rev. Sci. Instrum.* **84**, 083704 (2013).
- [13] Takaki, Y., Kawai, H., and Ohzu, H., “Hybrid holographic microscopy free of conjugate and zero-order images,” *App. Opt.* **38**, 4990–4996 (1999).